Cardiovascular Research (2010) **87**, 578–584
doi:10.1093/cvr/cvq059

Astroglia are a possible cellular substrate of angiotensin(1-7) effects in the rostral ventrolateral medulla

Fang Guo[1†], Beihui Liu[2†], Feige Tang[2], Samantha Lane[2], Ekaterina A. Souslova[3], Dmitriy M. Chudakov[3], Julian F.R. Paton[2], and Sergey Kasparov[2*]

[1]Department of Pharmacology, Hebei Medical University, Shijiazhuang 050017, China; [2]Department of Physiology and Pharmacology, Bristol Heart Institute, School of Medical Sciences, University of Bristol, Bristol BS8 1TD, UK; and [3]Institute of Bioorganic Chemistry RAS, Miklukho-Maklaya 16/10, Moscow 117997, Russia

Received 15 September 2009; revised 17 February 2010; accepted 19 February 2010; online publish-ahead-of-print 3 March 2010

Time for primary review: 20 days

Aims Angiotensin(1-7) (Ang1-7) acting at the level of the rostral ventrolateral medulla (RVLM) affects arterial pressure. The cellular substrate of Ang1-7 remains unknown. We sought to determine which cell types in RVLM could mediate its actions and whether these are altered in the spontaneously hypertensive rat (SHR).

Methods and results Astrocytes, catecholaminergic (CA-ergic) and non-CA-ergic neurones were targeted with adenoviral vectors in organotypic slice cultures from Wistar rats and SHR. Astrocytic Ca^{2+} signalling was monitored using a genetically engineered Ca^{2+} sensor Case12. CA-ergic neurones expressed enhanced green fluorescent protein (EGFP) under control of the PRS × 8 promoter, whereas non-CA-neurones expressed EGFP under control of the synapsin-1 promoter. Neurones were recorded in whole cell mode while $[Ca^{2+}]_i$ was monitored using Rhod-2. RVLM astrocytes responded to Ang1-7 (200–1000 nM) with concentration-dependent $[Ca^{2+}]_i$ elevation. In SHR, the response to 1000 nM was significantly attenuated. The competitive Ang1-7 receptor antagonist A779, but not the AT_1 receptor blocker (losartan), suppressed Ang1-7-induced $[Ca^{2+}]_i$ elevations, which were also antagonized by blocking intracellular Ca^{2+} stores. Ang1-7 evoked no consistent changes in $[Ca^{2+}]_i$ or membrane excitability in CA-ergic or non-CA-ergic neurones in either rat strain.

Conclusion Astroglia are a plausible cellular target of Ang1-7 in RVLM. Our data suggest that astrocytic responsiveness to Ang1-7 is reduced in SHR. We hypothesise that Ang1-7 modulates astrocytic signalling which *in vivo* may affect local metabolism and microcirculation, resulting in changes in activity of RVLM pre-sympathetic neurones and hence blood pressure.

Keywords Astroglia • Ca^{2+} sensor Case12 • Angiotensin(1-7) • Rostral ventrolateral medulla • Spontaneously hypertensive rat • Catecholaminergic neurones • Non-catecholaminergic neurones

1. Introduction

Angiotensin(1-7) (Ang1-7) has emerged as an important component of the renin–angiotensin system in both peripheral tissues and the central nervous system.[1,2] Ang1-7 is a product of the reaction catalysed by angiotensin-converting enzyme type 2 (ACE-2) and is thought to act via a G-protein coupled Mas receptor.[3] In peripheral tissues, Ang1-7 counteracts many effects of angiotensin II[4] and its over-expression in the vascular endothelium of the stroke-prone spontaneously hypertensive rat (SHR) reduces endothelial dysfunction and blood pressure and also improves haemodynamics.[5,6] However, the Mas receptor is also expressed in the brain where immunofluorescence was particularly evident in many areas associated with cardiovascular homeostasis, including the nucleus of the solitary tract, caudal, and rostral ventrolateral medulla (RVLM), paraventricular and supraoptic hypothalamic nuclei.[7] Acute microinjections of Ang1-7 into the ventral medulla have been shown to trigger cardiovascular responses. In anaesthetized rabbits, injections

† The first two authors contributed equally to the study.

* Corresponding author. Tel: +44 117 3312275; fax: +44 117 3312288, Email: sergey.kasparov@bristol.ac.uk

Published on behalf of the European Society of Cardiology. All rights reserved. © The Author 2010. For permissions please email: journals.permissions@oxfordjournals.org.

into the RVLM were pro-hypertensive, whereas injections into more caudal parts of the ventrolateral medulla decreased blood pressure and heart rate.[8] In un-anaesthetized normotensive rats microinjections of Ang1-7 into RVLM also resulted in an increase in blood pressure but, interestingly this effect was absent in animals subject to mild physical exercise.[9] Yamazato *et al.*[10] chronically over expressed ACE-2 in the ventrolateral medulla of the rat using viral vectors with the aim to produce a lasting increase in Ang1-7 synthesis. In the SHR, this resulted in a gradual reduction in mean arterial pressure (significant after 4th week), although the same procedure had no detectable effect in normotensive Wistar-Kyoto rats.[10]

Taken together these observations indicate that Ang1-7 has important modulatory effects on central autonomic control of arterial pressure and that one site of its action in the brain is the RVLM. However, the cellular substrate through which Ang1-7 mediates its effects in the RVLM remains elusive. The objective of this study was therefore to identify which of the three cell types most abundant in the RVLM [e.g. catecholaminergic (CA-ergic) neurones, non-CA-ergic neurones, and astrocytes] are responsive to the acute application of Ang1-7 and whether any Ang1-7 effects are altered in the SHR. The reason for looking at the ventral medullary CA-ergic neurones specifically is that these neurones are widely implicated in control of sympathetic outflow and, therefore of cardiovascular homeostasis (reviewed by Dampney *et al.*[11] and Guyenet[12]). Several recent studies suggest an important contribution of RVLM glutamatergic neurones to the maintenance of sympathetic outflow.[11,13,14] Finally, astrocytes have recently emerged as an active component of various complex central mechanisms and it is now clear that their role in the brain is by no means limited to just providing structural and metabolic support to neurones. Astrocytes can affect neuronal activity in a variety of ways. This may include release of glutamate, ATP, or other signalling molecules. Moreover, one most intriguing feature of these cells is their ability to regulate microcirculation and participate in coupling of neuronal activity and local blood flow.[15–17]

In this study, we have adopted a novel technical approach based on targeted expression of genes in the above-mentioned three key cellular populations in question: CA-ergic neurones, non-CA-ergic neurones, and astrocytes. For this purpose, we used adenoviral vectors (AVV) with cell-specific promoters. In addition, we introduce here a novel genetic tool for Ca^{2+} imaging in astroglia AVV-sGFAP-Case12.

2. Methods

Animal procedures were carried out according to the United Kingdom Home Office Guidelines on Animals (Scientific Procedures) Act of 1986, consistent with the Guide for the Care and Use of Laboratory Animals published by the US National Institutes of Health (NIH Publication No. 85-23, revised 1996) and approved by the University of Bristol Ethical Review Group (UB/05/035). In total, approximately 45 Wistar rats (WR) and 20 SHR pups were used, animals were originally purchased from Harlan UK.

2.1 Viral-cell type targeting strategy

To target the three chosen different cell types we used AVV with cell-specific promoters. In order to study effects of Ang1-7 specifically in astrocytes, we have generated a novel vector AVV-sGFAP-Case12, where a recently described genetically encoded Ca^{2+} sensor Case12[18] is expressed under control of a transcriptionally enhanced compact promoter of the glial acidic fibrilatory protein, GFAP.[19]

CA-ergic neurones were made fluorescent by exposing slices to the AVV-PRS × 8-enhanced green fluorescent protein (EGFP).[20] From the previous studies, we know that PRS × 8 drives expression in many CA-ergic nuclei such as locus coeruleus,[20] A2 and RVLM.[21] We have also demonstrated directly using micro-amperometry that PRS × 8 targeted cells in RVLM slices are releasing catecholamines and therefore are from C1 and possibly A1 cell groups. Finally, we took advantage of the previously found feature of the human synapsin-1 promoter, which drives expression in many neuronal types and is highly selective for neurones over astroglia, but is almost inactive in CA-ergic neurones.[21] Thus, when slices were exposed to AVV-sSYN-EGFP, fluorescent neurones could be expected to be glutamatergic or possibly of some other type, excluding CA-ergic. In AVV-sSYN-EGFP, transcriptional amplification strategy was applied to synapsin-1 to increase the level of transgene expression.[19] To confirm that AVV with PRS × 8 and sSYN promoters target different neuronal types, we have transduced cultured slices ($n = 6$) with a mixture of AVV-PRS × 8-DsRed2 and AVV-sSYN-EGFP. Slices were then imaged 7–8 days later in the same way as those used for recordings (Supplementary material online, *Figure S1A–C*). Out of the total 153 neurones (seven fields of view from six slices), we only found three cells (<2%) with a clear co-localization of DsRed2 and EGFP (Supplementary material online, *Figure S1D*; those are likely to be cholinergic neurones from the nucleus ambiguous which occasionally migrate towards the edge of the slices and are sensitive to both promoters). Hence, our sampling errors in terms of distinguishing between local CA-ergic neurones (able to activate PRS × 8 promoter) and non-CA-ergic neurones (where SYN promoter is active) is negligible.

2.2 Generation of AVV-sGFAP-Case12 and AVV-sSYN-EGFP

To construct the AVV-sGFAP-Case12 shuttle vector pXcX-mCMV/GfaABC1D-Case12, a lentiviral shuttle vector pTYF-mCMV/GfaABC1D-Case12 was first made by replacing the *Spe*I/*Not*I EGFP fragment in pTYF-mCMV/GfaABC1D-EGFP[19] with *Nhe*I/*Not*I Case12 fragment from pCase12.[18] The I-*Sce*I fragment from pTYF-mCMV/GfaABC1D-Case12 containing the expression cassette mCMV/GfaABC1D-Case12 was then swapped into the same sites of the pXcX-Sw-linker which then was recombined into an adenoviral vector named AVV-sGFAP-Case12. To produce the AVV-sSYN-EGFP shuttle vector pXcX-mCMV/SYN-EGFP, I-*Sce*I fragment from pTYF-mCMV/SYN-EGFP[19] harbouring mCMV/SYN-EGFP expression cassette was swapped into the I-*Sce*I sites of pXcX-Sw-linker which then was recombined into an adenoviral vector named AVV-sSYN-EGFP.

2.3 Slice culture and viral transduction

As described previously,[22,23] 7 to 9-day-old Wistar or SHR pups were sacrificed by halothane overdose and used to prepare 250 μm brainstem slices. Slices were cut rostrally to obex (a few more caudal slices were also used, see below) under sterile dissection solution, plated onto Millipore membranes and kept at the interface between the feeding medium (pH 7.3) and humidified atmosphere (5% CO_2, 37°C). For experiments with astrocytes, OPTI-MEM-based medium was used. For imaging neurones, Neurobasal-based culturing medium was employed. In both cases, the medium was changed three times a week. Cultures were used for experiments between 7 and 14 days *in vitro*. AVV were added to the media at the time of plating as described before.[24]

2.4 Ca^{2+} imaging and patch clamp

For recording, slices and underlying membrane were transferred into a recording chamber where they were continuously superfused by either bicarbonate-based artificial cerebro-spinal fluid (ACSF), as in[22] or HEPES-buffered ACSF. We have not noticed any obvious difference in basal properties of the cells or their responses to drugs with these

different types of ACSF and therefore the data are pooled. Ca^{2+} imaging in astrocytes was carried out using time-lapse mode (every 2 s) using a Leica confocal SP1 scanner with 488 nm excitation. Intensity of the laser was kept to the minimum to avoid quenching of the Case12 fluorescence. Electrophysiological recordings and Ca^{2+} imaging of selected neurones were carried out as described before.[22,25] Briefly, EGFP-fluorescent neurones were visualized using 488 nm light, patched with pipettes filled with Rhod-2 (0.5 mM) and recorded in current-clamp mode using a SEC-05LX amplifier (NPI, Germany). The data were acquired and analysed using Spike2 software (Cambridge Electronic Design, UK). Green laser light (543 nm) was used to excite Rhod-2. Changes of $[Ca^{2+}]_i$ in individual cells were assessed by changes in relative fluorescence intensity (F/F_0, where F indicates peak fluorescence intensity and F_0 denotes resting fluorescence intensity measured before the arrival of the drug in the recording chamber).

2.5 Drugs and their application

After a stabilization period of at least 10 min, drugs were added into the perfusion medium and the effects were observed during a 5 min period. AngII, 2-Aminoethyl diphenyl borate (2-APB), cyclopiazonic acid (CPA), and ATP-K salt were from Sigma (UK). Ang1-7 was from Bachem (UK) and Ang1-7 antagonist A779 was from GeneScript Corp (USA). Losartan was a gift from Merk, Sharp, and Dohme. Rhod-2 (tripotassium salt) was supplied by Cambridge Bioscience (UK). In some neurones, 600 and 1000 nM concentrations of Ang1-7 were applied sequentially after a 5–10 min wash.

2.6 Calculations and statistics

All values in this text are mean ± SEM, n refers to the total number of cells in each population unless stated otherwise. Ca^{2+} responses to Ang1-7 in astrocytes widely varied in their amplitude, time course, and overall shape of response, making meaningful evaluation of these parameters difficult. Therefore, for evaluation purposes, we decided to disregard the apparent magnitude of Ca^{2+} change in individual astrocytes but base our statistics on a fraction of the responsive cells. The threshold was set to 10% of the baseline fluorescence intensity and the cells where application of a drug resulted in a timely (within first 60 s after the drug arrival into the chamber) elevation in $[Ca^{2+}]_i$ were counted as 'responders'. We then applied Fisher's exact test as implemented in GraphPad Prism software. In each case, the values were calculated based on experiments from three to six individual slices from different batches; with the total number of cells studied for each condition was >50. We also measured the amplitude of responses in these cells (data not shown) and this evaluation demonstrated the same trends as results presented in the text.

Neuronal $[Ca^{2+}]_i$ and electrophysiological parameters were evaluated using standard approaches[22] and differences were examined using Student's paired t-test. Statistical evaluation was carried out using Microsoft Excel and GraphPad Prism 4.

3. Results

3.1 AVV-sGFAP-Case12 as a Ca^{2+} sensor in astroglia

Astrocytic $[Ca^{2+}]_i$ are known to be highly variable and it was therefore beneficial to use a method which would visualize this process in large numbers of these cells selectively, excluding neurones. To that end, we have generated AVV-sGFAP-Case12, its map is shown in *Figure 1A*. The initial characterization of Case12 in cell lines was published earlier.[18] Application of AVV-sGFAP-Case12 to organotypic slice cultures led to the expression of bright fluorescence in numerous astrocytes across various areas of the slice (*Figure 1B*). In order to further confirm the specificity of AAV-sGFAP-Case12 to astroglia, immunofluorescent staining of the ventral medulla from rats injected with this vector was performed, essentially as previously described.[19] Case12 (green) was well co-localized with GFAP staining (red), consistent with previous reports (*Figure 1C*). In accordance with previous observations, Case12 was photostable only at moderate levels of illumination and therefore for time-lapse imaging laser intensity was kept at low levels to avoid quenching. As this vector has not been used for imaging astrocytes before, it was important to obtain an estimate of the response which could be anticipated when the cells were maximally activated. We therefore applied 100 μM of ATP, one of the strongest activators of the astrocytic Ca^{2+} signalling, to three slice cultures. As shown in *Figure 1D* and *E*, ATP resulted in a characteristic Ca^{2+} response in 55% of astrocytes with an average increase of fluorescence intensity of 65%, although some individual cells exhibited Ca^{2+} elevations in excess of 300%. Thus, AVV-sGFAP-Case12 is a highly sensitive genetic tool for imaging changes in $[Ca^{2+}]_i$ in astroglia. Its sensitivity compares with that of a conventional chemical indicator Rhod-2 (Supplementary material online, *Figure S2*).

3.2 Effects of Ang1-7 on astrocytes

Only in the slices containing the rostral ventral medulla could the responses to Ang1-7 (200, 600, 1000 nM) be detected. Cells in slices at the level of the obex and caudal to it were essentially non-responsive (five slices, $n > 50$ data not shown).

Ang1-7 (200, 600, 1000 nM) triggered intracellular Ca^{2+} elevations or waves in 6–41% of WR astrocytes, the response was maximal at 600 nM. Thus, the difference between the effect of 200 and 600 nM was highly significant, but between 600 and 1000 nM was not, in spite of an obvious trend (*Figure 2A*). Interestingly, there was a lower incidence of intracellular Ca^{2+} elevations in astrocytes in response to Ang1-7 in SHR compared with astrocytes from WR. This difference was significant at 1000 nM ($P < 0.05$; *Figure 2A*). Ang1-7 induced fairly slow $[Ca^{2+}]_i$ elevations which in some cells was maintained even after the drug was discontinued (*Figure 2B*). Ang1-7 antagonist A779 (200 μM) blocked the effect of Ang1-7 in WR astrocytes ($P < 0.01$, $n = 64$, *Figure 2C*). On the other hand, the AT_1 receptor blocker losartan (1 μM) did not attenuate the response to 600 nM Ang1-7 ($P > 0.1$, $n = 84$, *Figure 2C*).

Two intracellular Ca^{2+} store antagonists, 2-APB (100 μM) and CPA (10 μM) were used to test whether the effect of Ang1-7 is store dependent. Slices were pre-incubated in these drugs for 5 min after which Ang1-7 600 nM was co-infused. In both cases, Ang1-7 effects were strongly attenuated ($P < 0.05$, $n = 89$ and $n = 72$ correspondingly, *Figure 2C*). Therefore, Ca^{2+} elevations evoked by Ang1-7 are likely to involve Ca^{2+} release from intracellular stores.

3.3 Neurones

In slices from normotensive WR animals Ang1-7 (200–1000 nM) had essentially no effect on either CA-ergic (PRS × 8 targeted) or non-CA-ergic (SYN targeted) neurones in RVLM slices prepared exactly like those for imaging astrocytes in terms of $[Ca^{2+}]_i$ (*Figure 3A*) or resting membrane potential (RMP) (*Figure 3B*). Similarly, in slices prepared from SHR, Ang1-7 200 nM had no significant effects on either $[Ca^{2+}]_i$ or RMP (*Figure 4*; $P > 0.1$ in all cases). In a few additional experiments, higher concentrations of Ang1-7 (600 and 1000 nM) were tested on neurones in SHR slices but no clear effects were detected in either case. Passive membrane resistance also did not change (data not shown). L-glutamate washed at the

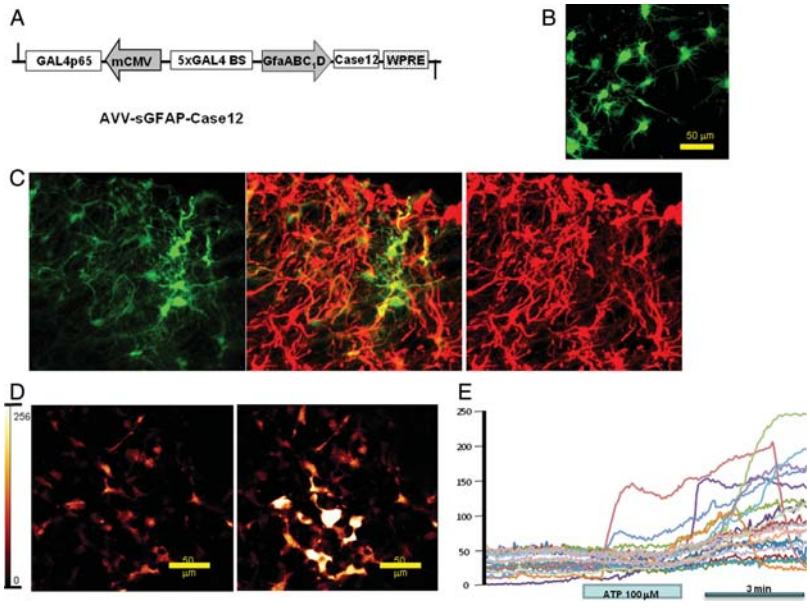

Figure 1 Characterization of the novel $[Ca^{2+}]_i$ imaging tool, AVV-sGFAP-Case12. (*A*) Layout of the AVV-sGFAP-Case12. Note that minimal CMV core promoter (mCMV) fused in the antisense orientation to the compact astroglial promoter ($GfaABC_1D$) serves to co-express an artificial transcriptional enhancer Gal4p65. For details see Liu *et al.*[19] (*B*) Case12 expressing astrocytes in an organotypic cultured slice from the rat medulla. (*C*) In order to additionally confirm the specificity of AAV-sGFAP-Case12 to astroglia, immunofluorescent staining of the ventral medulla from rats injected with this vector was performed; essentially as previously described (refer Liu *et al.*[19] for details). Case12 (green) was well co-localized with GFAP staining (red), consistent with previous reports. Image size: 250 × 250 µm. (*D*) Case12 responds with a strong increase in fluorescence intensity to the application of ATP (100 µM). Left image: before infusion of ATP; right image: 3 min after initiation of ATP application. (*E*) Traces of fluorescent intensity measurements from several astrocytes after stimulation with ATP. Note that Case12 has an unprecedented dynamic range and in some cells fluorescence intensity increases by 300% and more.

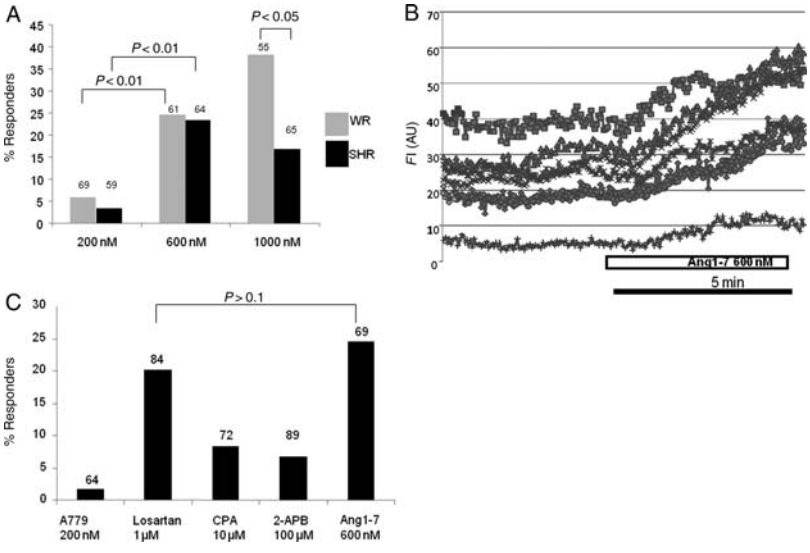

Figure 2 Ang1-7 effects on astrocytes imaged within the RVLM in organotypic cultured slices of rat medulla. (*A*) Ang1-7 (200–1000 nM) causes a dose-dependent activation of astrocytes in RVLM in WR (grey bars) and SHR (black bars). Statistics are based on the fraction of activated astrocytes from the total number of recorded cells as indicated on the top of the bars. (*B*) Example of an Ang1-7-induced Ca^{2+} response in astrocytes. Ang1-7 induced fairly slow $[Ca^{2+}]_i$ elevations which in some cells could last for a long time even after the drug was discontinued. (*C*) Pharmacological analysis of Ang1-7 effect. The concentration of 600 nM was used in all these experiments. Note that Ang1-7 effect was blocked by a competitive blocker of the Mas receptor A779 but not losartan, the Ang II antagonist. Two blockers of intracellular stores, CPA, and 2-APB significantly ($P < 0.05$) attenuated the effect of Ang1-7. The right bar represents the effect of 600 nM Ang1-7 alone for comparison.

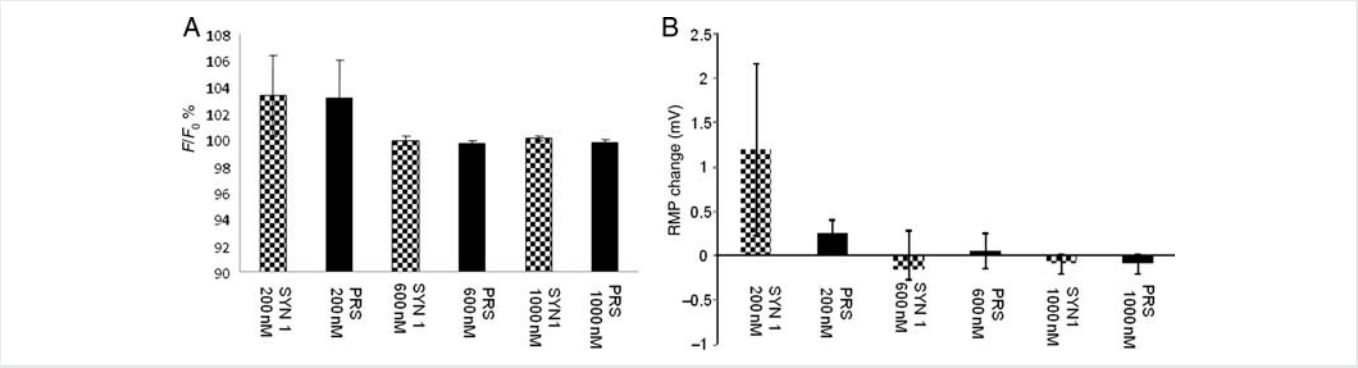

Figure 3 Ang1-7 (200–1000 nM) has no significant effects on either CA-ergic or non-CA-ergic neurones in WR. Ang1-7 effects on $[Ca^{2+}]_i$, (*A*) and the RMP (*B*). CA-ergic neurones were targeted with viruses containing PRS × 8 promoter (black bars), non-CA-ergic neurones were targeted with vectors with sSYN promoter (patterned bars). Concentrations of Ang1-7 are shown next to the bars. Neither parameter was significantly affected at any concentration ($P > 0.1$ in all cases). Six to eight neurones were used for each measurement. Note that at the end of the recording we verified that the cells were viable and the infusion was functional using a standard agonist (L-glutamate).

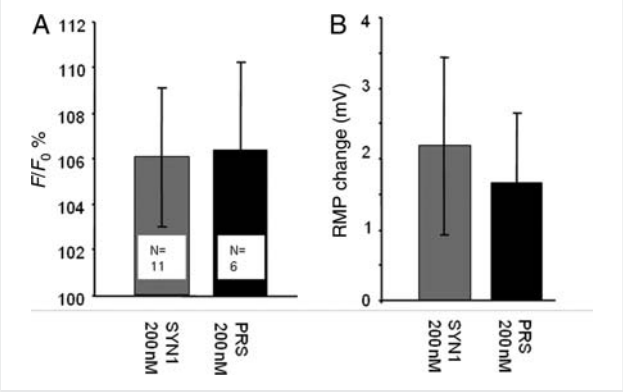

Figure 4 Ang1-7 (200 nM) has no significant effects on either CA-ergic or non-CA-ergic neurones in SHR. Slices were treated the same way as *Figure 3*. Ang1-7 was without effect on these neurones ($P > 0.1$ in all cases), numbers of cells indicated on the plot.

end of the experiments as a positive control evoked robust $[Ca^{2+}]_i$ increases (Supplementary material online, *Figure S3*) and depolarizations (Supplementary material online, *Figure S4*).

4. Discussion

This study used an innovative approach to identify a cellular substrate of Ang1-7 in the ventral medulla of rats, by selectively targeting the three most abundant cell types in that part of the brain—astroglia, CA-ergic neurones and non-CA-ergic neurones with cell-specific viral vectors. We found that the only cellular compartment that responded to Ang1-7 was astroglia, while we could not detect any consistent evidence of neuronal activation or inhibition.

Although many studies suggest that Ang1-7 has central effects,[9,26–31] the cellular substrate of its action in the CNS remains elusive. Several studies have identified the ventrolateral medulla as a site where Ang1-7 has important effects on the cardiovascular system. For example, microinjections of Ang1-7 into the RVLM produced significant increases in arterial pressure.[32] Interestingly, equimolar doses of Ang1-7 in the caudal ventrolateral medulla produced a depressor effect similar to that evoked by angiotensin II and this effect was of comparable magnitude in WR and SHR.[33] Overexpression of ACE-2 on RVLM of SHR caused a long-lasting hypotensive effect.[10] The mechanism behind this effect of ACE-2 was not identified in these experiments, but the authors proposed that it may be the result of faster AngII degradation, rather than a direct effect of Ang1-7. Thus, these results do not directly conflict with the previously mentioned data obtained using acute Ang1-7 microinjections, but rather suggest that chronic effects of ACE-2 *in vivo* may involve more than one mechanism and possibly other cell types than neurones.

RVLM harbours a variety of cellular types which could all be responsible for Ang1-7 actions. The most prominent of the neuronal populations in that area are CA-ergic neurones from the C1 adrenergic and A1 noradrenergic clusters surrounded by non-CA-ergic neurones, many of which use glutamate as the main transmitter.[11,13,14] In addition, as in virtually any other part of the brain, astroglia are also highly abundant. In order to understand how Ang1-7 mediates its central effects on arterial pressure, it is essential to localize the cellular substrate of its action as an initial first step. In this study, we have used the strategy of selectively targeting three plausible cell types with cell-specific viral vectors. For visualizing astrocytic Ca^{2+} signalling, we selectively targeted astrocytes with a recently described genetically engineered Ca^{2+} sensor Case12[18] using transcriptionally amplified glial fibrillitary protein promoter.[19] This approach allows monitoring astrocytic $[Ca^{2+}]_i$ without the need to either patch the cells or bulk load them with esters of Ca^{2+}-sensitive dyes that are non-selective for any specific cell type. In contrast, cell-specific expression of a Ca^{2+} sensor ensured that the fluorescent signal came from astroglia. We first established that the Case12 sensor has a very high dynamic range, consistent with previous observations[18] using ATP as a positive control. Ang1-7 had a concentration-dependent effect on astrocytic Ca^{2+} and at 1000 nM ~40% of WR astrocytes were excited by it. Interestingly, SHR astrocytes responded to 200 and 600 nM Ang1-7 in a similar way, but the highest concentration (1000 nM) was significantly less effective (*Figure 2A*), suggesting that SHR Ang1-7 signalling might be compromised, although as long as we do not know the actual physiological range of Ang1-7 in the brain, this remains a speculation. The effect of Ang1-7 was specific and obviously mediated

by Mas receptor because A799 almost completely eliminated it, while AT_1 receptor blocker losartan was without effect (*Figure 2C*). In addition, Ca^{2+} was released at least in part from the intracellular stores because pre-incubation with CPA and 2-APB strongly attenuated the effect of 600 nM Ang1-7.

Astrocytes are rapidly emerging as a very important component of central homeostatic mechanisms.[34] Previously, it was demonstrated that in human astrocytoma cell lines, Ang1-7 stimulated release of prostaglandin but caused no consistent effects on intracellular Ca^{2+}[35]. The lack of Ca^{2+} responses in that previous study could be explained by the differences between the astrocytic cell lines and astrocytes studied within their usual cellular environment albeit in organotypic slices. Moreover, it is not impossible that there are regional differences in astrocytic $[Ca^{2+}]_i$ sensitivity to Ang1-7, at least in our experiments we could only obtain reliable $[Ca^{2+}]_i$ responses in slices cut at the locations corresponding to the rostral, rather than caudal VLM (data not shown). However, our study is consistent with that of Tallant *et al.*[35] in that astrocytes are sensitive to Ang1-7 and therefore could potentially mediate its actions in the brain. How exactly Ang1-7 actions on astrocytes may be converted into changes in neuronal activity affecting autonomic homeostasis such as changes in sympathetic outflow is not known at present. One particularly interesting possibility is that by modulating astrocytes, Ang1-7 could affect microcirculation within the brain. Indeed, several recent studies have established a functional link between astrocytic activity and brain microvessels (reviewed by Iadecola and Nedergaard[16]). It was demonstrated that under the conditions when oxygen levels are low and astrocytic Ca^{2+} signalling is elevated, astrocytes can release lactate. Lactate then attenuates a transporter-mediated prostaglandin E2 uptake from the extracellular space and the accumulating prostaglandin causes vasodilatation.[15] If Ang1-7 is able to facilitate astrocytic Ca^{2+} signalling in RVLM as suggested by our data and, in addition stimulates prostaglandin release,[35] it could play a role in controlling microcirculation in this critical area of the brain. In this way, Ang1-7 could play a role in the control of sympathetic outflow and blood pressure, which would be consistent with the reported beneficial effect of ACE-2 overexpression in RVLM of SHR.[10]

Finally, we studied the effects of Ang1-7 on CA-ergic and non-CA-ergic neurones in RVLM slice cultures. For studies of CA-ergic neurones, we used a previously tested approach[22] based on EGFP expression in these cells with AVV bearing an artificial PRS × 8 promoter.[20,36] To label non-CA-ergic neurones, we took advantage of a previously identified feature of the SYN-1 promoter which was inactive in CA-ergic neurones.[21] The fact that SYN-1 targets a different population of neurones from PRS × 8 was verified in this study directly (Supplementary material online, *Figure S1*). The EGFP-positive neurones were recorded using patch pipettes and filled with Rhod-2 for Ca^{2+} imaging. However, we were unable to demonstrate direct effects of Ang1-7 on either CA-ergic or non-CA-ergic neurones in RVLM of either WR (200–1000 nM) or SHR by looking at the changes in the electrical behaviour of the neurones or their $[Ca^{2+}]_i$. The methods used here were indentical to those in our previous study where these neurones did respond to Ang II[22] and we confirmed that the cells were viable in the present experiments using L-glutamate at the end of the recording. It is therefore hard to imagine that the lack of Ang1-7 effects in the present experiments is a technical artefact. Yamazato *et al.*[10] also noted that in their hands Ang1-7 had no effect on neuronal activity, although did not show the actual data. Thus, the neuronal substrate for the acute pressure responses reported after Ang1-7 microinjections in this area, as reported by Silva *et al.*[32] remains unclear. In summary, the present results suggest that astroglia could be the key cellular compartment mediating Ang1-7 actions on cardiovascular homeostasis at the level of RVLM.

Supplementary material

Supplementary material is available at *Cardiovascular Research* online.

Conflict of interest: none declared.

Funding

F.G. was supported by the KC Wong fellowship from the Royal Society of the UK. B.L. and S.K. are supported by the British Heart Foundation RJ/07/006. F.T. is funded by Wellcome Trust (080314). S.L. is a recipient of PhD studentship from the BBSRC. E.A.S. and D.M.C. were supported by MCB RAS, RFBR UK 09-04-92603-KOa, Rosnauka 02.512.12.2053. J.F.R.P. was in receipt of a Royal Society Wolfson Research Merit Award.

References

1. Benter IF, Diz DI, Ferrario CM. Cardiovascular actions of angiotensin(1-7). *Peptides* 1993;**14**:679–684.
2. Chappell MC. Emerging evidence for a functional angiotensin-converting enzyme 2--angiotensin-(1-7)-MAS receptor axis: more than regulation of blood pressure? *Hypertension* 2007;**50**:596–599.
3. Santos RA, Simoes e Silva AC, Maric C, Silva DM, Machado RP, de Buhr I *et al.* Angiotensin-(1-7) is an endogenous ligand for the G protein-coupled receptor Mas. *Proc Natl Acad Sci USA* 2003;**100**:8258–8263.
4. Sampaio WO, Henrique deCC, Santos RA, Schiffrin EL, Touyz RM. Angiotensin-(1-7) counterregulates angiotensin II signaling in human endothelial cells. *Hypertension* 2007;**50**:1093–1098.
5. Alenina N, Xu P, Rentzsch B, Patkin EL, Bader M. Genetically altered animal models for Mas and angiotensin-(1-7). *Exp Physiol* 2008;**93**:528–537.
6. Rentzsch B, Todiras M, Iliescu R, Popova E, Campos LA, Oliveira ML *et al.* Transgenic angiotensin-converting enzyme 2 overexpression in vessels of SHRSP rats reduces blood pressure and improves endothelial function. *Hypertension* 2008;**52**:967–973.
7. Becker LK, Etelvino GM, Walther T, Santos RA, Campagnole-Santos MJ. Immunofluorescence localization of the receptor Mas in cardiovascular-related areas of the rat brain. *Am J Physiol Heart Circ Physiol* 2007;**293**:H1416–H1424.
8. Potts PD, Horiuchi J, Coleman MJ, Dampney RAL. The cardiovascular effects of angiotensin-(1-7) in the rostral and caudal ventrolateral medulla of the rabbit. *Brain Res* 2000;**877**:58–64.
9. Becker LK, Santos RA, Campagnole-Santos MJ. Cardiovascular effects of angiotensin II and angiotensin-(1-7) at the RVLM of trained normotensive rats. *Brain Res* 2005;**1040**:121–128.
10. Yamazato M, Yamazato Y, Sun C, ez-Freire C, Raizada MK. Overexpression of angiotensin-converting enzyme 2 in the rostral ventrolateral medulla causes long-term decrease in blood pressure in the spontaneously hypertensive rats. *Hypertension* 2007;**49**:926–931.
11. Dampney RA, Horiuchi J, Tagawa T, Fontes MA, Potts PD, Polson JW. Medullary and supramedullary mechanisms regulating sympathetic vasomotor tone. *Acta Physiologica Scandinavica* 2003;**177**:209–218.
12. Guyenet PG. The sympathetic control of blood pressure. *Nature Rev Neurosci* 2006;**7**:335–346.
13. Mayorov DN, Head GA. Glutamate receptors in RVLM modulate sympathetic baroreflex in conscious rabbits. *AM J Physiol-Reg I* 2003;**284**:R511–R519.
14. Stornetta RL, Sevigny CP, Schreihofer AM, Rosin DL, Guyenet PG. Vesicular glutamate transporter DNPI/VGLUT2 is expressed by both C1 adrenergic and nonaminergic presympathetic vasomotor neurons of the rat medulla. *J Comp Neurol* 2002;**444**:207–220.
15. Gordon GR, Choi HB, Rungta RL, Ellis-Davies GC, MacVicar BA. Brain metabolism dictates the polarity of astrocyte control over arterioles. *Nature* 2008;**456**:745–749.
16. Iadecola C, Nedergaard M. Glial regulation of the cerebral microvasculature. *Nature Neurosci* 2007;**10**:1369–1376.
17. Girouard H, Iadecola C. Neurovascular coupling in the normal brain and in hypertension, stroke, and Alzheimer disease. *J Appl Physiol* 2006;**100**:328–335.
18. Souslova EA, Belousov VV, Lock JG, Strɪmblad S, Kasparov S, Bolshakov AP *et al.* Single fluorescent protein-based Ca2+ sensors with increased dynamic range. *BMC Biotechnol* 2007;**7**:37.

19. Liu BH, Paton JFR, Kasparov S. Viral vectors based on bidirectional cell-specific mammalian promoters and transcriptional amplification strategy for use *in vitro* and *in vivo*. *BMC Biotechnol* 2008;**8**:49–56.
20. Hwang DY, Carlezon WA Jr, Isacson O, Kim KS. A high-efficiency synthetic promoter that drives transgene expression selectively in noradrenergic neurons. *Human Gene Therapy* 2001;**12**:1731–1740.
21. Lonergan T, Teschemacher AG, Hwang D-Y, Kim K-S, Pickering AE, Kasparov S. Targeting brainstem centres of cardiovascular control using adenoviral vectors: impact of promoters on transgene expression. *Physiol Genomics* 2005;**20**:165–172.
22. Teschemacher AG, Wang S, Raizada MK, Paton JFR, Kasparov S. Area-specific differences in transmitter release in central catecholaminergic neurons of spontaneously hypertensive rats. *Hypertension* 2008;**52**:1–8.
23. Teschemacher AG, Paton JFR, Kasparov S. Imaging living central neurones using viral gene transfer. *Adv Drug Deliv Rev* 2005;**57**:79–93.
24. Teschemacher AG, Wang S, Lonergan T, Duale H, Waki H, Paton JFR *et al*. Targeting specific neuronal populations in the brainstem using adeno- and lentiviral vectors: applications for imaging and studies of cell function. *Exp Physiol* 2005;**90**:61–69.
25. Wang S, Teschemacher AG, Paton JF, Kasparov S. Mechanism of nitric oxide action on inhibitory GABAergic signaling within the nucleus tractus solitarii. *FASEB J* 2006;**20**:1537–1539.
26. Hocht C, Gironacci MM, Mayer MA, Schuman M, Bertera FM, Taira CA. Involvement of angiotensin-(1-7) in the hypothalamic hypotensive effect of captopril in sinoaortic denervated rats. *Regul Pept* 2008;**146**:58–66.
27. Hellner K, Walther T, Schubert M, Albrecht D. Angiotensin-(1-7) enhances LTP in the hippocampus through the G-protein-coupled receptor Mas. *Mol Cell Neurosci* 2005;**29**:427–435.
28. Silva AQ, Santos RA, Fontes MA. Blockade of endogenous angiotensin-(1-7) in the hypothalamic paraventricular nucleus reduces renal sympathetic tone. *Hypertension* 2005;**46**:341–348.
29. Gironacci MM, Valera MS, Yujnovsky I, Pena C. Angiotensin-(1-7) inhibitory mechanism of norepinephrine release in hypertensive rats. *Hypertension* 2004;**44**:783–787.
30. Diz DI, Pirro NT. Differential actions of angiotensin II and angiotensin-(1-7) on transmitter release. *Hypertension* 1992;**19** (Suppl. 2):II41–II48.
31. Sakima A, Averill DB, Gallagher PE, Kasper SO, Tommasi EN, Ferrario CM *et al*. Impaired heart rate baroreflex in older rats: role of endogenous angiotensin-(1-7) at the nucleus tractus solitarii. *Hypertension* 2005;**46**:333–340.
32. Silva LC, Fontes MA, Campagnole-Santos MJ, Khosla MC, Campos RR Jr, Guertzenstein PG *et al*. Cardiovascular effects produced by micro-injection of angiotensin-(1-7) on vasopressor and vasodepressor sites of the ventrolateral medulla. *Brain Res* 1993;**613**:321–325.
33. Ferreira PM, Alzamora AC, Santos RA, Campagnole-Santos MJ. Hemodynamic effect produced by microinjection of angiotensins at the caudal ventrolateral medulla of spontaneously hypertensive rats. *Neuroscience* 2008;**151**:1208–1216.
34. Allen NJ, Barres BA. Neuroscience: Glia—more than just brain glue. *Nature* 2009;**457**:675–677.
35. Tallant EA, Jaiswal N, Diz DI, Ferrario CM. Human astrocytes contain two distinct angiotensin receptor subtypes. *Hypertension* 1991;**18**:32–39.
36. Kasparov S, Teschemacher AG, Hwang D-Y, Kim K-S, Lonergan T, Paton JFR. Viral vectors as tools for studies of central cardiovascular control. *Prog Biophys Mol Bio* 2004;**84**:251–277.